Effect of Ionomer on Clay Dispersions in Polypropylene-Layered Silicate Nanocomposites

Hongzhi Liu, Hyung Tag Lim, Kyung Hyun Ahn, Seung Jong Lee

School of Chemical and Biological Engineering, Seoul National University, Seoul 151-744, Korea

Received 4 September 2006; accepted 16 December 2006
DOI 10.1002/app.26036
Published online in Wiley InterScience (www.interscience.wiley.com).

ABSTRACT: In this study, polypropylene (PP)/clay nanocomposites containing different concentrations of ethylene-methacrylic acid ionomer (i.e. Surlyn®) were prepared, and the effect of ionomer on clay dispersion was studied via WAXD, rheology, SEM, and TEM. The role of the ionomer in the nanocomposites was compared with that of maleic anhydride grafted PP (PP-*g*-MA), which has been widely used as a compatibilizer in making PP/clay nanocomposites. With an increase in the concentration of compatibilizer, the position of d_{001} peak of OMMT shifted toward a lower angle for PP-*g*-MA system, while the position remained almost unchanged for Surlyn system, in which a larger interlayer spacing (d_{001}) was found with respect to the former. In rheology, the addition of the ionomer led to a gradual increase in both moduli and complex viscosity, and the nonterminal behavior at low frequency was observed in both systems. In addition, the ternary hybrid containing 20 wt % Surlyn achieved the largest enhancement in relative viscosity, which was more than that of the nanocomposite prepared from pure Surlyn or pure PP, presumably indicative of the existence of strong interaction between the components. Finally, SEM and TEM micrographs demonstrated that exfoliated structure was preferred for PP/Surlyn/OMMT hybrids, while intercalated morphology for PP/PP-*g*-MA/OMMT. © 2007 Wiley Periodicals, Inc. J Appl Polym Sci 104: 4024–4034, 2007

Key words: nanocomposites; dispersion; PP; ionomer; clay; hybrids

INTRODUCTION

Since the outstanding performance of nylon-6/montmorillonite nanocomposite was first reported by Toyota group in 1993,[1–4] there have been plenty of works on polymer–clay nanocomposites. It is now widely recognized that the exfoliated structure would contribute to the maximum performance enhancement. Polypropylene (PP) is one of the most important commodity thermoplastics and the PP-clay nanocomposite (PPCN) appears to be very attractive and promising. Thus, great efforts were dedicated to the preparation of PPCN. However, it is still a great challenge to prepare PPCN with well-exfoliated structure until now because of the incompatibility of the hydrophobic polymer with hydrophilic silicates, even though the commercial clays available are normally modified with long chain alkyl ammonium salts via ion-exchange reaction. That is, a strong polarity still remains even for the organically modified clay. At present, the most successful alternative is the addition of maleic anhydride grafted PP (PP-*g*-MA) as a compatibilizer during melt blending.[5–7] Indeed, the presence of the functionalized graft-copolymer facilitates the dispersion of clay platelets remarkably. Several studies revealed that the density of MA groups had a strong effect on the final morphology and properties of the composite.[5,8–11]

Unfortunately, the same expected improvement in properties (e.g., mechanical properties) as PA6 nanocomposites has not yet been achieved for PP. Two aspects may be responsible for this failure.[8,12] One is still lower degree of exfoliation, the other is high loading of PP-*g*-MA to achieve the desired degree of exfoliation, which in turn partly compromises the final mechanical properties due to the inferior properties of the copolymer used.

As a class of representative ionomer, Surlyn® developed by the Dupont company is an ethylene-*co*-methacrylic acid (E-MAA) polymer, in which a small amount of methyl-carboxylic acid introduced as a comonomer are partially neutralized by metal bases, e.g., Na^+, Li^+, and Zn^{2+}. As a result, the ionic groups associate with each other and form ion-rich domains of nanometer size (i.e. ionic aggregates) within the resulting polymer matrix. Compared with the host polymer PE, the formation of ionic aggregates markedly improves the material performance, e.g., superior abrasion resistance, transparency, scratch and scuff resistance, low temperature impact resistance, chemical resistance, melt strength, and adhesion properties, and so on. In addition, owing to its unique molecular

Correspondence to: K. H. Ahn (ahnnet@snu.ac.kr).
Contract grant sponsor: Korea Energy Management Corp. (KEMCO); contract grant number: 2005-*R*-NM01-P-01-2-400-2005.

Journal of Applied Polymer Science, Vol. 104, 4024–4034 (2007)

TABLE I
Characteristics of Materials Used

Name	Trademark	Characteristics	Supplier
PP	HP562T	MFR (230°C, 2.16 kg) = 6.0 g/min, M_w = 127,000, M_n = 13,000	Polymirae Company Ltd (Korea)
Ionomer	Surlyn®8945	MFR(190°C, 2.16 kg) = 4.5 g/10 min, specific gravity = 0.96, methacrylic acid content = 15.2, sodium content = 1.99 wt %, neutralization = ~40%[22]	DuPont company in Korea
PP-*g*-MA	Polybond®3200	MFR (190°C, 2.16 kg) = 11.5 g/min M_w = 4,000, MA content = 1.0 wt %, T_m = 163°C, T_d = 325°C[8]	Crompton Corp. Middlebury, USA
OMMT	Cloisite®20A (i.e. Dimethyl bis(hydrogenated-tallow) ammonium montmorillonite)	CEC = 95 meq/100 g, organic content = 39.6 wt %	Southern Clay Products

structure, this ionomer has been often used as a compatibilizer for blends of PP and polar polymers, e.g., PP/PBT,[13] PP/nylon,[14–16] PP/Liquid crystalline polymers (LCPs),[17] and PP/EVOH[18–20].

The presence of the pendant ionic groups in the ionomer creates favorable interactions between the ionomers and the aluminosilicate clays. There have been several reports related to the nanocomposites prepared from ionomers, e.g., Surlyn,[21,22] PBT ionomer,[23] PET ionomer,[24] polyethylene-base ionomer,[25] and isobutylene-based ionomer[26]. It was demonstrated that the remarkable improved exfoliation was successfully achieved with respect to the corresponding nonionic polymers. To our knowledge, however, very few works focused on the effect of the addition of ionomers on clay dispersion in polymer–clay nanocomposites.[27]

In this work, PPCNs containing poly(ethylene-*co*-methacrylic acid) ionomer, (i.e., Surlyn8945) were prepared via direct melt intercalation in an intermeshing, corotating twin-screw extruder. Our main purpose is to preliminarily examine the effects of the added Surlyn on clay dispersion of PPCNs. For the purpose of comparison, the widely used PP-*g*-MA (Polybond3200) was used as a reference.

EXPERIMENTAL

All the materials used were commercial products, among which the Surlyn was kindly provided from the DuPont Company. The molecular structure of Surlyn is shown as follows:

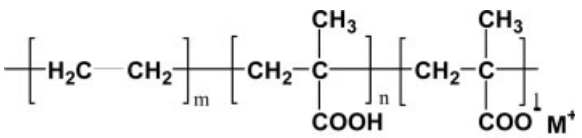

$M^+ = Na^+, Zn^{2+}, Li^+$

where m, n, and l are the number of each segment unit, respectively.

In this work, the choice of Cloisite®20A as an organoclay was based on the previous results, in which the surfactant structure was correlated with the degree of exfoliation in the nanocomposites based on Surlyn[21] and LLDPE.[28] The studies revealed that higher levels of organoclay exfoliation could be achieved using the surfactants with multiple alkyl tails on the ammonium ion rather than one tail. This was believed to be as a result of better affinity of the ionomers for the highly aliphatic organic modifier than for the pristine surface of the clay. In addition, the larger the number of alkyl tails, the more the silicate surface was shielded from the matrix. These combined factors resulted in better exfoliation of the organoclay having multiple alkyl tails. The specific characteristics of the above materials are summarized in Table I. The content of OMMT is expressed in terms of parts per hundred resins (phr; including PP and Surlyn), and fixed at 5 phr in this study. For brevity, PPxCN and PPxMCN represent PP/Surlyn/OMMT hybrids and PP/PP-*g*-MA/OMMT, respectively. Among them, the number x refers to the concentration of the added Surlyn or PP-*g*-MA, while SurlynCN denotes the clay nanocomposites prepared from pure Surlyn.

Prior to compounding, all the raw materials were dried in a vacuum oven at 80°C for a minimum of 12 h. Melt compounding was performed using an intermeshing, corotating twin-screw extruder (Bautek, Korea) with a screw speed of 100 rpm. The temperature profile from hopper to die was set at 120/120/170/180/190/190/170/170°C. As a reference, pure PP, Surlyn, and their binary blends were also extruded under the same condition, respectively. For morphological and property characterization, the pellets were compression-molded into the disks with a diameter of 25 mm

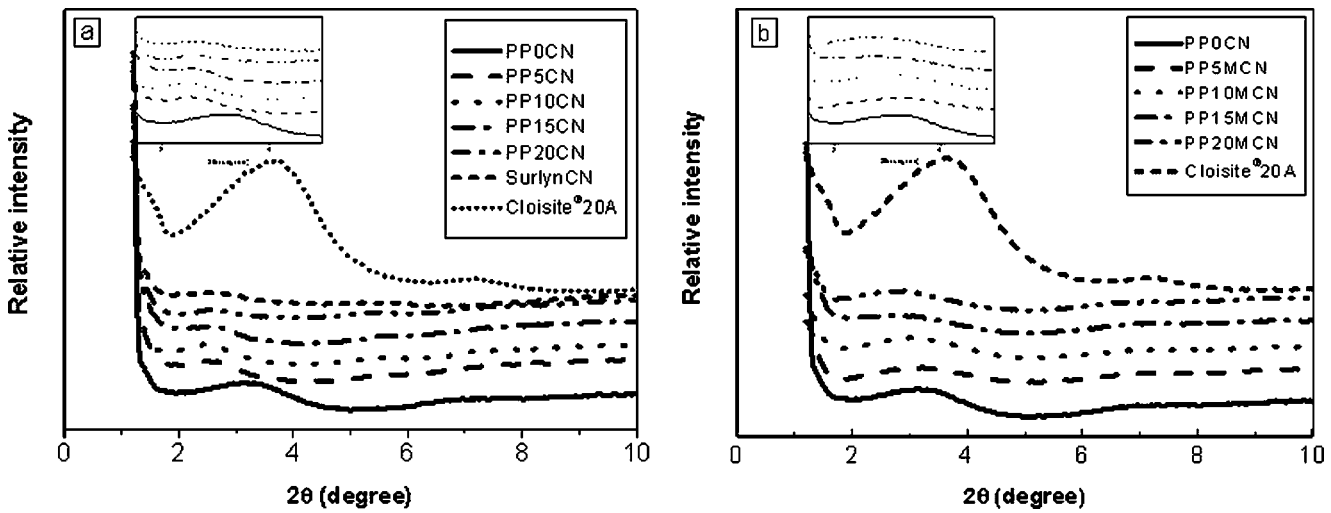

Figure 1 WXRD profiles for PP/PP-*g*-MA/OMMT (a) and PP/Surlyn/OMMT (b), respectively. Insert: the magnification of the d_{001} diffraction peak of OMMT.

and a thickness of ~1 mm using a hot press (Carver, CH4386) at 190°C.

Characterization

Wide angle X-ray data were collected on Rigaku D/MAX-IIIC X-ray diffractometer (Cu Kα radiation, wavelength = 1.5418) with accelerating voltage of 40 kV. Diffraction spectra were obtained over a 2θ range of 1.2°–10°. Rheological measurements were performed in a small amplitude oscillatory shear mode on a parallel-plate rheometer (Rheometrics, RMS800), using discs with 25 mm diameter and 1 mm thickness. Storage (G') and loss modulus (G'') were measured over a frequency range of 0.1–100 rad/s at 180°C in a nitrogen environment. Prior to frequency sweep, a strain sweep test was performed to ensure that the strain used was within the linear viscoelastic range. The morphology of the samples was examined using a field-emission scanning electron microscope (FE-SEM; JSM-6700F, JEOL) and a high resolution transmission electron microscope (HR-TEM; JEM-3010, JEOL), respectively. The fractured surfaces for FE-SEM imaging were prepared by cryogenic fracturing in liquid nitrogen and then sputter-coating with Pd. TEM observation was performed on cryo-ultramicrotomed sections at an acceleration voltage of 300 kV.

RESULTS AND DISCUSSION

WAXD

Figure 1(a) shows a series of X-ray diffraction patterns (XRD) of original OMMT and its hybrids with varying concentration of Surlyn. Meanwhile, the XRD patterns of the PP/PP-*g*-MA/OMMT nanocomposites are given in Figure 1(b) as a comparison. The calculated values of interlayer spacing (d_{001}) are summarized in Table II.

The interlayer spacing of Cloisite 20A is measured to be 2.36 nm before compounding. For the incompatibilized system (PP0CN), the WAXD pattern exhibits only a slight increase (about 0.4 nm) in the gallery height with respect to the original OMMT, which implies that only a small amount of PP could intercalate into the interlayer after melt extrusion. This result slightly differs from that reported for the same system prepared via internal mixer by other investigators,[9] who found no increase in the gallery spacing of OMMT. This discrepancy could be attributed to different processing conditions and different molecular weight of PP used. Therefore, such slight improvement does not necessarily mean that the

TABLE II
Interlayer Spacing for Composite Materials Calculated from WAXD Data

Designation	Formulation	d_{001}-spacing (nm)
OMMT	–	2.36
PP/Surlyn/OMMT		
PP0CN	100/0/5	2.79
PP5CN	95/5/5	3.55
PP8CN	92/8/5	3.52
PP10CN	90/10/5	3.51
PP15CN	85/15/5	3.37
PP20CN[a]	80/20/5	3.45
SurlynCN[a]	0/100/5	3.37
PP/PP-*g*-MA/OMMT		
PP5MCN	95/5/5	2.74
PP10MCN	90/10/5	2.95
PP15MCN	85/15/5	3.06
PP20MCN	80/20/5	3.03

[a] The exact peak position is difficult to precisely determine due to broad distribution of the peak.

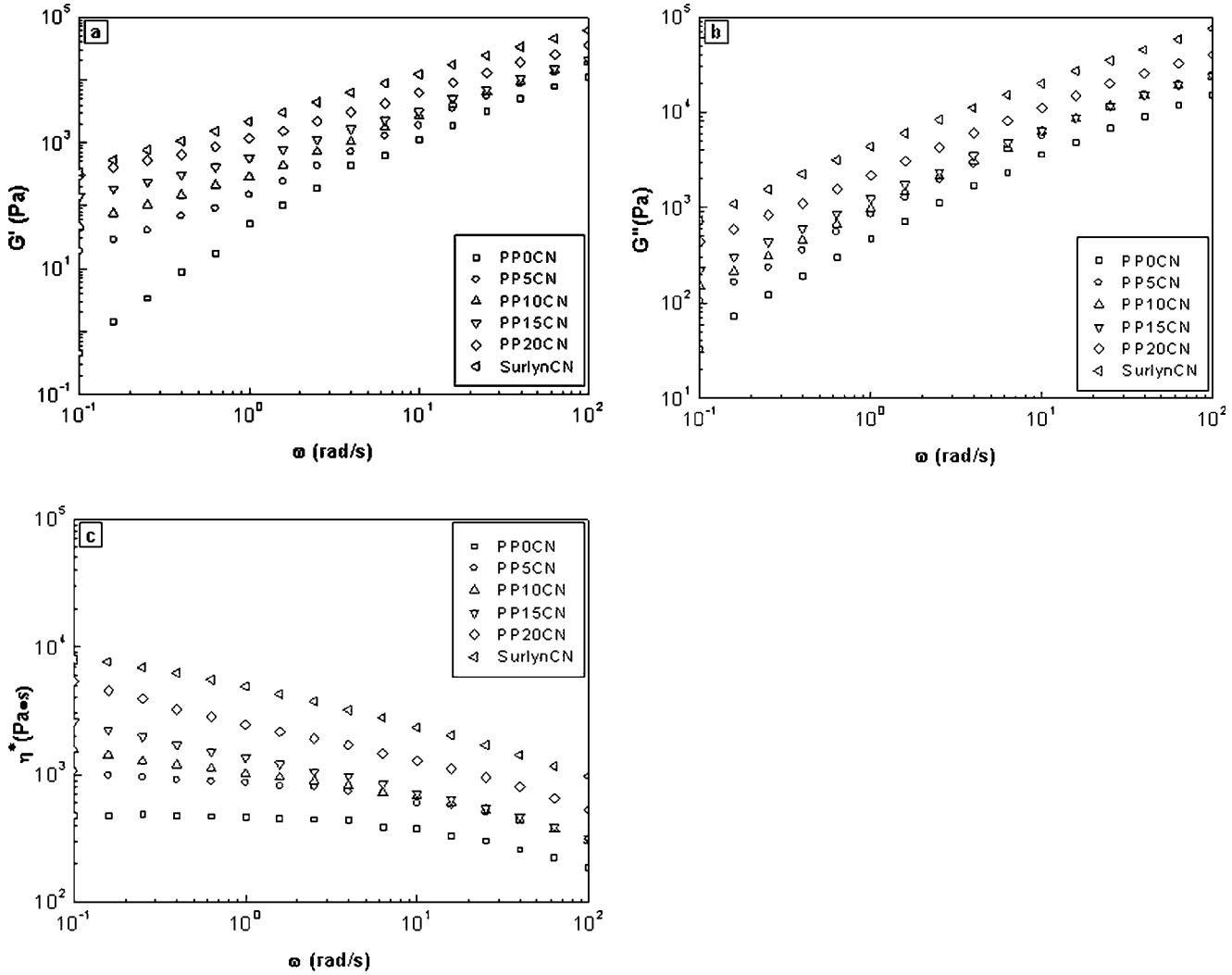

Figure 2 Rheological data of PP/Surlyn/OMMT hybrids at 180°C: (a) storage modulus (G'); (b) loss modulus (G''); (c) complex viscosity (η^*).

intercalation process is favorable for our case over the other in the nonpolar PP systems.

In contrast, the effect of added Surlyn on the interlayer spacing of OMMT is remarkable, as shown in Figure 1(b). When only 5 wt % Surlyn was added into PP/clay composites, the peak of the {001} basal diffraction of organoclay shifted to a lower angle, indicating an increase in interlayer spacing by the intercalation process. However, upon further addition of Surlyn, the position of the characteristic peak remains unchanged, which is quite different from the results observed in the PP/PP-*g*-MA/OMMT nanocomposites [Fig. 1(b)]. In the latter, the basal diffraction peak slowly shifts toward a lower angle with increasing PP-*g*-MA content. This tendency is coincident with other reports of the same system.[9] However, it should be noted that the former system exhibits a larger basal spacing (d_{001}) than the latter, thus suggesting better intercalation effect for PP/Surlyn/OMMT over PP/PP-*g*-MA/OMMT.

In addition, above 15 wt % of the ionomer, the d_{001} diffraction peak becomes broadening and its intensity is weaker. As a result, the well-defined interlayer spacing is difficult to be determined accurately. This result indicates that the stacks of layered silicates become more disordered, although a periodic distance is still maintained. In addition, the partial exfoliation of the layered silicates could be responsible for the decrease in intensity.

Rheological properties

WAXD can only detect the periodically stacked layers of the clay particles, i.e., the measurement of d_{001} spacing in the intercalated structure and little can be said about the spatial distribution of the clay particles.[29–31] It is well known that the rheological properties of the nanocomposites are sensitive to the state of dispersion of nano-fillers. So the rheological characterization may well be regarded as a sensitive

tool to reveal the global state of dispersion in the polymer-nanocomposites.[8,9]

Figure 2 shows moduli (G' and G'') and complex viscosity (η^*) of PP/Surlyn/OMMT nanocomposites with varying concentration of Surlyn at 180°C. When 5 wt % of the ionomer is added, a significant increase in both moduli and complex viscosity is observed, compared to the pure PP/OMMT composite (PP0CN). With the addition of Surlyn up to 15 wt %, the moduli at low frequency increase gradually with leveling off of the slope, indicative of the non-terminal behavior. One can also notice that a progressive increase in η^* value occurs at low frequency. In addition, the Newtonian plateau at low frequency range characteristic of the PP0CN sample weakens, and the yielding or shear-thinning phenomenon of η^* becomes more pronounced.

When the concentration of Surlyn reaches 20 wt %, however, the moduli increase significantly such that the magnitude of G' in PP20CN is almost comparable to that of Surlyn hybrids (i.e., SurlynCN) at low frequency. Moreover, its non-terminal behavior becomes even more prominent than the latter. Like moduli, the magnitude of η^* also begins to exhibit a dramatic increase at this concentration. These results presumably indicate the transformation from liquid-like to pseudo solid-like response.[32,33]

In view of higher η^* value for added Surlyn relative to PP matrix, the increase of η^* in PP/Surlyn/OMMT hybrids is related not only to the improved exfoliation of clay, but also to the addition of Surlyn itself. To isolate the effect of dispersion state of the nano-fillers, the relative viscosity (η_{rel}^*) has been defined as the magnitude of the complex viscosity, η_c^*, of the nanocomposites divided by the complex viscosity of the silicate-free matrix (i.e., PP, PP/Surlyn, and Surlyn as the matrix of PP0CN, PP/Surlyn/OMMT and SurlynCN, respectively), η_m^*. Figure 3 shows the relative viscosity of the above nanocomposites, in which there appears to be a monotonic increase in the magnitude of η_{rel}^* with the ionomer concentration in the range investigated. Therefore, it is reasonable to say that the degree of dispersion or exfoliation increases with the increase in Surlyn concentration. It is worth noting that the largest enhancement in the relative viscosity is observed for the PP nanocomposites with the highest loading of Surlyn (i.e., PP20CN) rather than the SurlynCN sample. Since the complex viscosity of SurlynCN is higher than that of PP20CN, such higher η_{rel}^* value for the latter could result from the increased interfacial contribution between PP and Surlyn components. The subsequent microscopic observation demonstrates that some of the silicate layers locate at the interface between PP and Surlyn for PP/Surlyn/OMMT hybrids, as will be shown later in Figure 8. Very recently, the role of interfacial activation or compatibilization of clay layers at

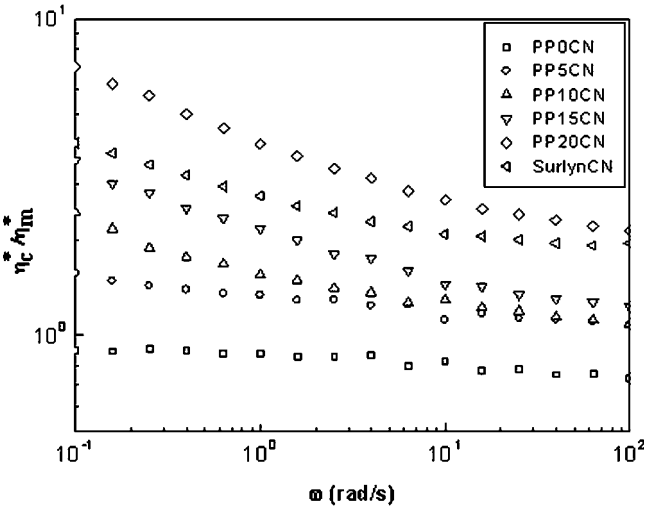

Figure 3 Relative complex viscosity of PP/Surlyn/OMMT hybrids at 180°C.

the interphase has been widely confirmed in many polymer blends.[34–38] Therefore, we expect that there also exists the same interfacial activity in our system. However, further investigation will be necessary to have a clear understanding on the relationship between morphology and rheology.

As a comparison, Figure 4 shows rheological properties as a function of frequency for PP hybrids containing different concentrations of PP-*g*-MA. As expected, the addition of PP-*g*-MA results in a remarkable increase in the rheological properties of PP hybrid. At low frequency region, the slope of moduli decreases gradually and shear-thinning behavior of η^* becomes more pronounced, as the content of PP-*g*-MA further increases. At high frequency (above 10 rad/s), however, the moduli of the hybrids remain almost unaffected by the addition of PP-*g*-MA up to 20 wt %, which differs from the results observed in the corresponding PP/Surlyn/OMMT samples above. This observation reflects the difference in the relaxation response of the polymer chains in the region of high frequency.

Terminal slopes of G' and G'' for all silicate hybrids at low frequency are summarized in Table III. Without the addition of Surlyn, PP0CN shows a typical terminal behavior close to $G' \propto \omega^2$ and $G' \propto \omega$. In close analogy to PP/PP-*g*-MA/OMMT, the terminal behavior of G' and G'' for PP/Surlyn/OMMT hybrids exhibits the power-law dependence with the slope much smaller than two and one, respectively. Furthermore, like PP/PP-*g*-MA/OMMT nanocomposites, a gradual decrease in the power-law dependence of G' and G'' is observed with increasing Surlyn loading. The absence of terminal behavior is considered as a ''pseudosolid-like'' response, which arises from the formation of network structure.[39] Such a non-terminal behavior has also been observed in the

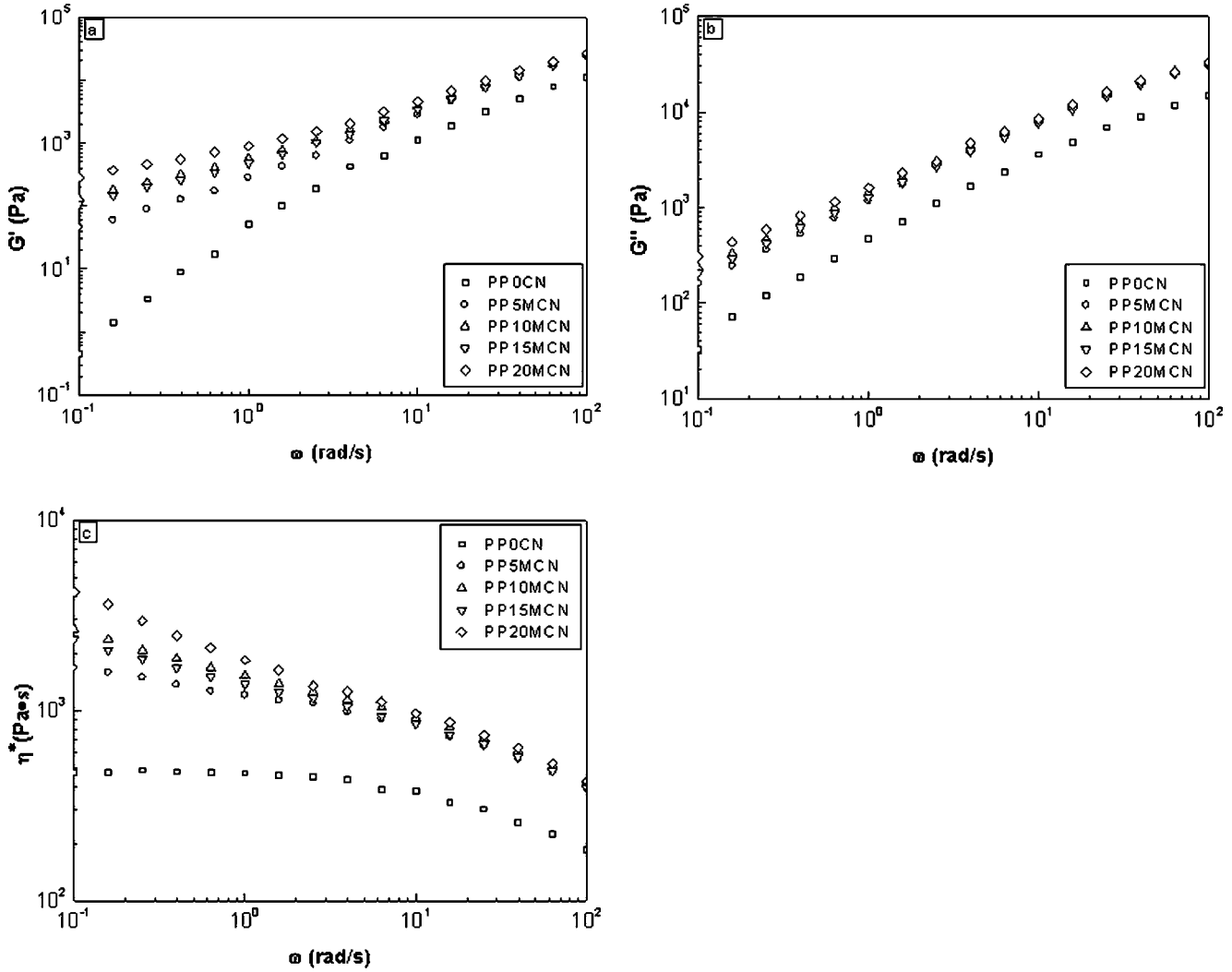

Figure 4 Rheological data of PP/PP-*g*-MA/OMMT hybrids at 180°C: (a) storage modulus (G'); (b) loss modulus (G''); (c) complex viscosity (η^*).

TABLE III
Terminal Slopes of G' and G'' for PP/Surlyn/OMMT and PP/PP-*g*-MA/OMMT Silicate Hybrids

Designation	Slope of G'	Slope of G''
PP/Surlyn/OMMT		
PP0CN	1.99	1.12
PP5CN	0.88	0.90
PP10CN	0.78	0.82
PP15CN	0.60	0.75
PP20CN	0.56	0.69
SurlynCN	0.79	0.78
PP/PP-*g*-MA/OMMT		
PP5MCN	0.79	0.85
PP10MCN	0.62	0.79
PP15MCN	0.63	0.79
PP20MCN	0.49	0.71

Terminal slopes were estimated for all samples at frequency below 1 rad/s.

systems with block copolymer or liquid-crystal.[40,41] All these rheological characteristics will be related to the microstructures, and detailed morphological differences will be provided in the following sections.

FE-SEM

To directly reveal the state of clay dispersion in the polymer matrix, SEM images of PP/Surlyn/OMMT and PP/PP-*g*-MA/OMMT hybrids are provided in Figures 5 and 6, respectively. In the case of uncompatibilized PP0CN, many clay tactoids can be clearly observed, as shown in Figure 5(a). Evidently, the failure of clay exfoliation in PP matrix is mainly responsible for the observation. However, clay tactoids are hardly distinguishable from the matrix upon the addition of Surlyn. This implies the remarkably improved dispersion of clays, which has been partly confirmed by XRD and rheology data.

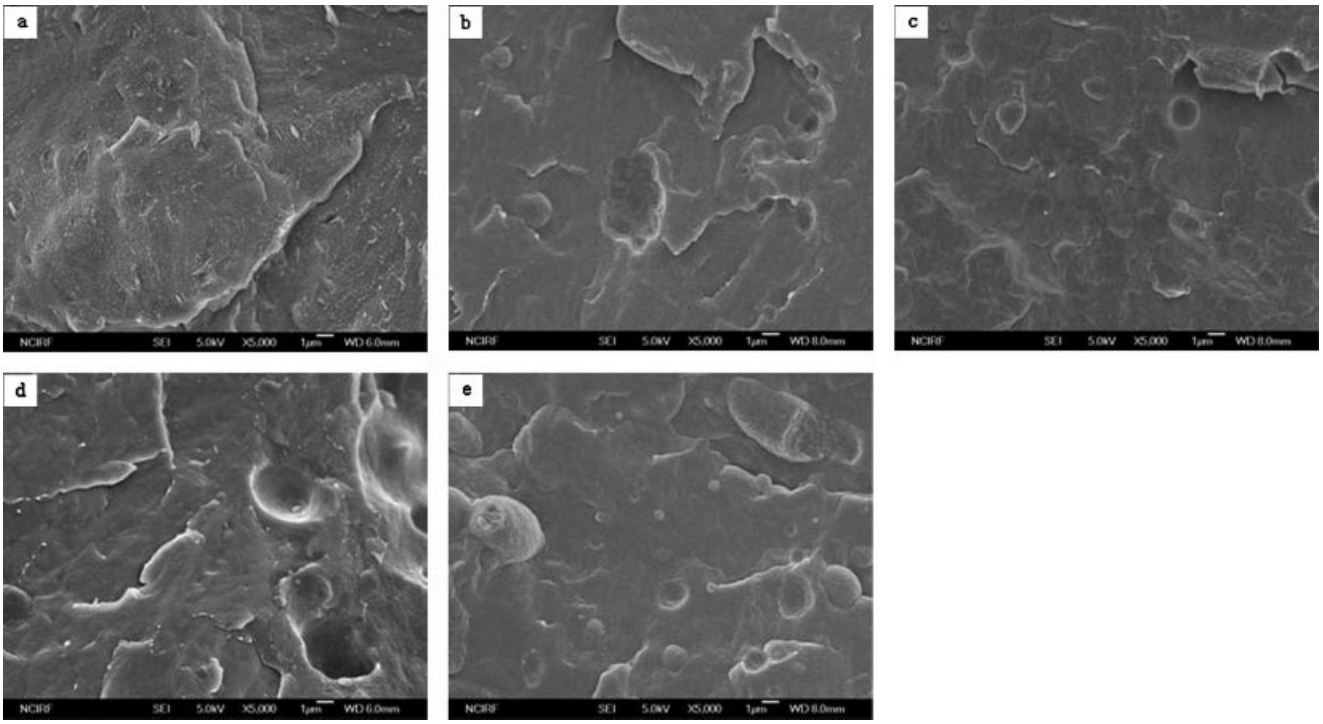

Figure 5 Cryo-fractured SEM micrographs of PP/Surlyn/OMMT hybrids: (a) 100/0/5; (b) 95/5/5; (c) 90/10/5; (d) 85/15/5; (e) 80/20/5.

On the other hand, the large difference can be found for PP/PP-*g*-MA/OMMT, compared to the PP/Surlyn/OMMT. In the former system, the clay tactoids are still visible, although the tactoid size is reduced with increasing PP-*g*-MA concentration (Fig. 6). This suggests that the intercalated structure prevails in the latter, while exfoliation or better dispersion does for the former.

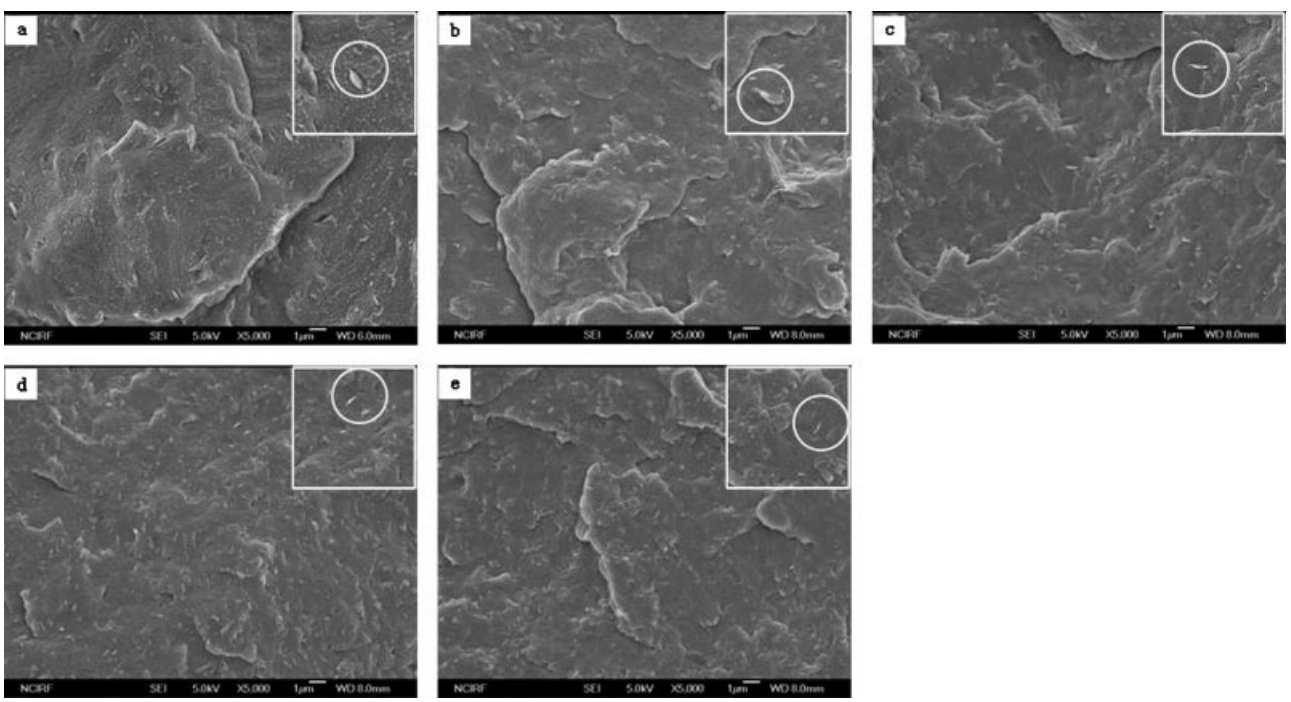

Figure 6 Cryo-fractured SEM micrographs of PP/PP-*g*-MA/OMMT hybrids: (a) 100/0/5; (b) 95/5/5; (c) 90/10/5; (d) 85/15/5; (e) 80/20/5. Inserts at right top of each picture indicate the presence of clay tactoids

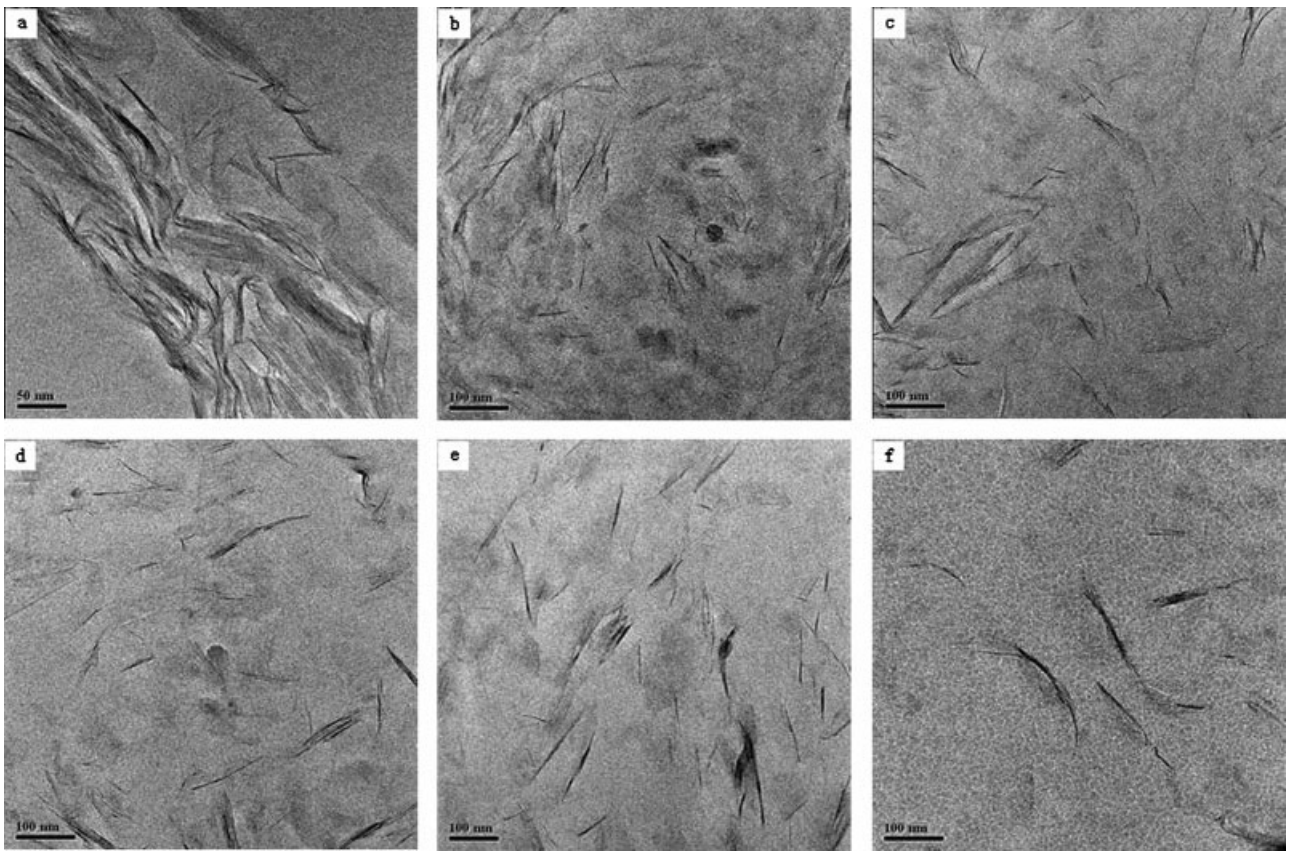

Figure 7 TEM micrographs of PP/Surlyn/OMMT hybrids at high magnification: (a) 100/0/5; (b) 95/5/5; (c) 90/10/5; (d) 85/15/5; (e) 80/20/5; (f) 0/100/5.

HR-TEM

As it is hardly possible to clearly image the exfoliated morphology of polymer–clay nanocomposites using SEM, TEM technique has been employed. Figure 7 first shows high-magnification TEM micrographs of PP/Surlyn/OMMT nanocomposites with varying concentration of Surlyn. Without the addition

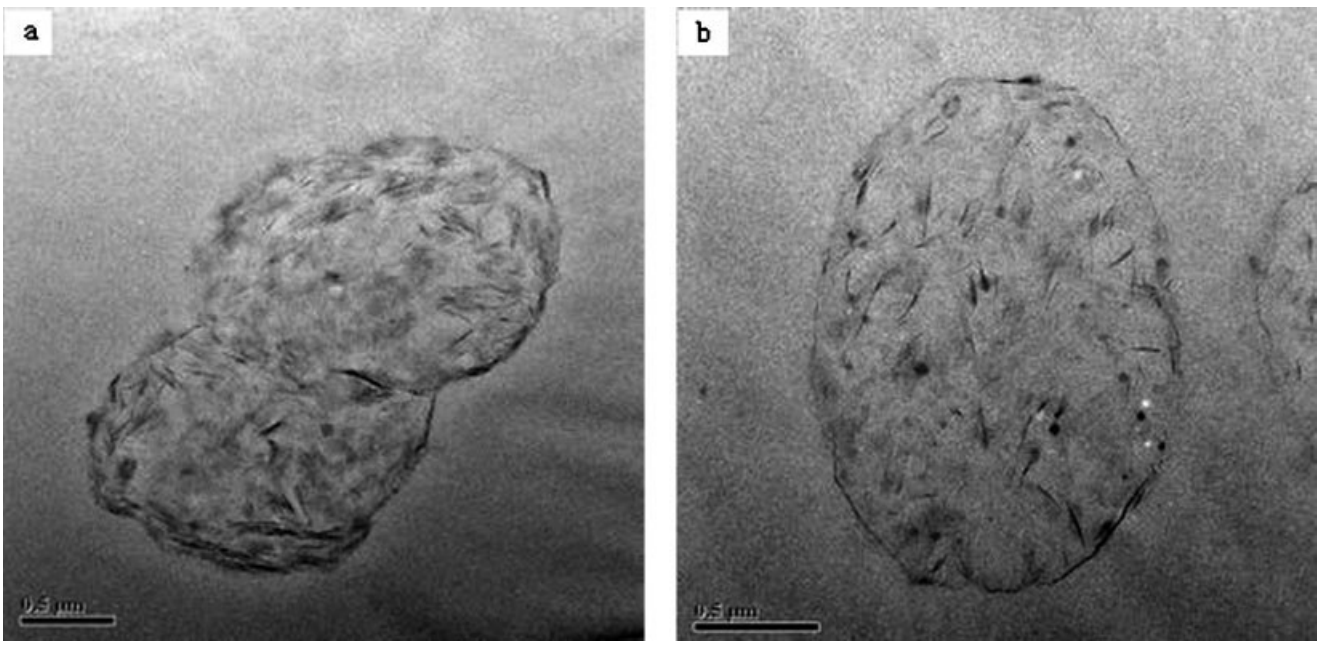

Figure 8 TEM micrographs of PP/Surlyn/OMMT hybrids at low magnification: (a) 95/5/5 and (b) 80/20/5.

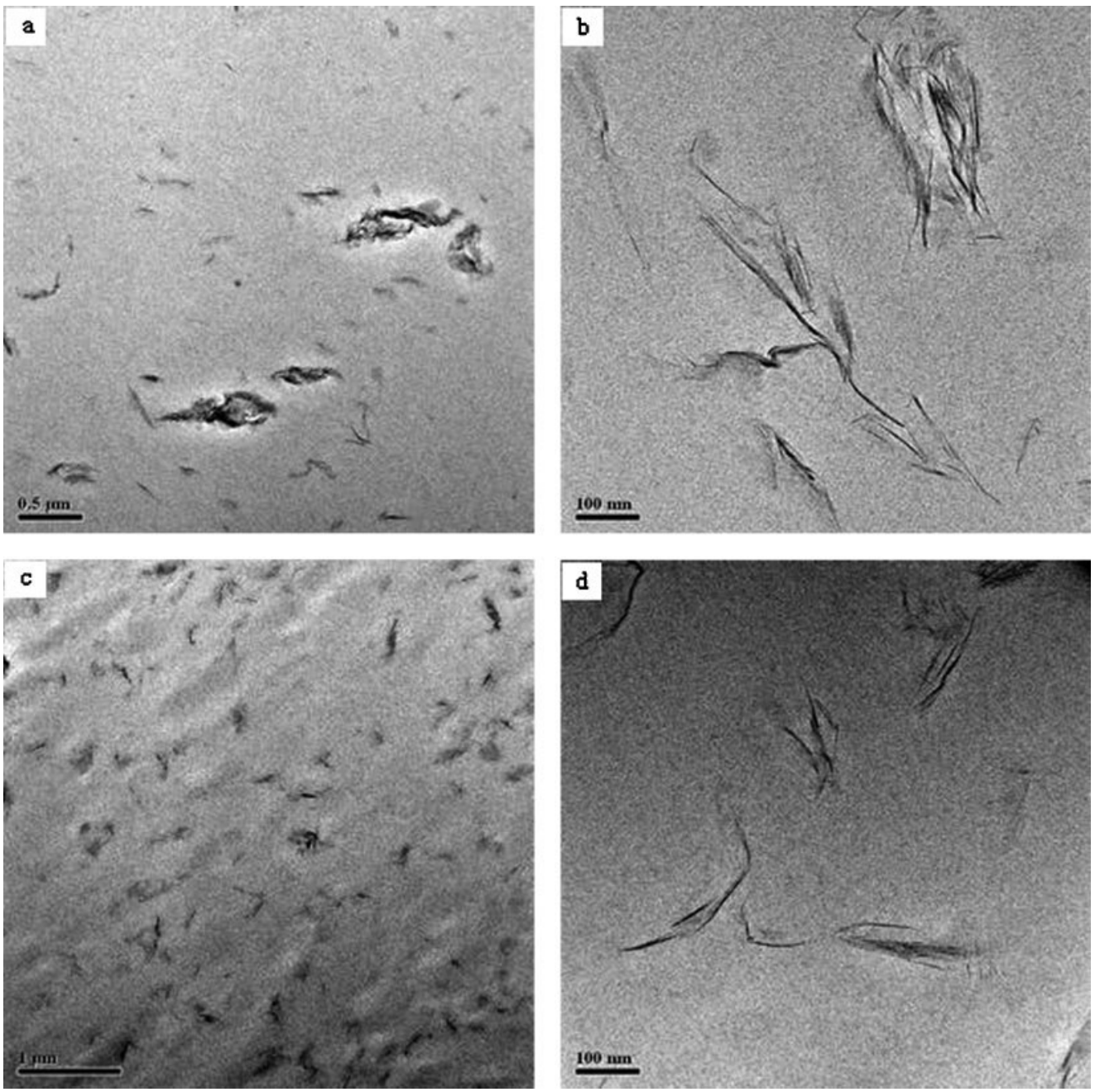

Figure 9 TEM micrographs of PP/PP-*g*-MA/OMMT hybrids: (a,b) 95/5/5; (c,d) 80/20/5. Left: low magnification; right: high magnification.

of Surlyn (i.e., PP0CN), there exist clay aggregates on a micrometer level with few separated silicate layers. When 5 wt % Surlyn is added, one can clearly observe that the size of silicates is greatly reduced and small aggregates consisting only of 2–5 individual layers are visible, corresponding to the partial exfoliation of the clays. Also, the amount of clay aggregates appears to decrease gradually with the increase of Surlyn content. In particular, in the case of PP20CN, the individual silicate layers become more prevalent. The above TEM images imply the progressively increased exfoliation of OMMT with the addition of ionomer. Here, it needs to be pointed out that the TEM observation for PP/Surlyn/OMMT hybrids is not contradictory to their aforementioned WAXD results. WAXD technique is useful to identify the ordered intercalated structure of clay, e.g., the measurement of *d*-spacing in intercalated structure. Unlike TEM, it can reflect little information about the exfoliation state or global distribution of silicate layers in the matrix. It has been reported that there can exist different degree of clay dispersion, even for polymer–clay

hybrids having similar interlayer spacing (d_{001}) of clay tactoids. Lee et al. prepared PP nanocomposites based on a modified organoclay with isobutyl trimethoxysilane to investigate the effects of such modifications of organoclay on the microstructure and properties of the nanocomposites.[30] TEM images revealed that the modification of the edges of clay platelets with organic silane resulted in a more uniform dispersion of clay platelets in PP matrix, while no difference of interlayer spacing (d_{001}) was found for both PP-clay nanocompsites via WAXD data. Interestingly, it can be further noticed that the silicate layers locate not only inside the dispersed domain but also at the interface, as evidenced in Figure 8.

As a comparison, the dispersion state of clays in the PP/PP-*g*-MA/OMMT hybrids is shown in Figure 9, in which intercalated structure is still more dominant compared to the analogue of PP/Surlyn/OMMT even at high PP-*g*-MA concentration. In addition, the selective localization of clay layers fails to be observed in the case of PP/PP-*g*-MA/OMMT hybrids. Therefore, the TEM analysis agrees well with the results from other measurements.

CONCLUSIONS

The effect of added Surlyn on clay dispersion of PP/clay hybrids was investigated with PP-*g*-MA as a comparison. WAXD data demonstrated that in the case of PP/Surlyn/OMMT, the d_{001} diffraction peak of PP-clay hybrid (i.e., PP0CN) was markedly shifted to a lower angle even when only 5 wt % Surlyn was added. However, upon further addition of Surlyn, the position of the diffraction peak remained unchanged. This trend was quite different from the results observed in the PP/PP-*g*-MA/OMMT hybrids, in which the diffraction peak slowly shifted to the lower angle with the concentration of PP-*g*-MA. Moreover, compared to the corresponding PP/PP-*g*-MA/OMMT hybrids, a larger interlayer spacing of clay was found for PP/Surlyn/OMMT hybrids. The linear viscoelastic properties demonstrated that the addition of Surlyn resulted in a progressive enhancement in both moduli and complex viscosity, which could be attributed to the effect induced by the improved clay dispersion based on the results of relative viscosity. In addition, like PP/PP-*g*-MA/OMMT, the nonterminal behavior at low-frequency was also observed for PP/Surlyn/OMMT hybrids, implying the formation of pseudo solid-like structure. SEM and TEM micrographs revealed that more intercalated structure was found in the PP/PP-*g*-MA hybrids compared to PP/Surlyn/OMMT, in which more exfoliated layers could be observed. Furthermore, the degree of exfoliation was found to increase with the content of added Surlyn, as evidenced in TEM pictures. However, it needs to be mentioned that the above discrepancy between TEM and WAXD results for PP/Surlyn/OMMT system resulted from different probing ability of both techniques in identifying either intercalation or exfoliation structure.

References

1. Fukushima, Y.; Okada, A.; Kawasumi, M.; Kurauchi, T.; Kamigaito, O. Clay Miner 1988, 23, 27.
2. Usuki, A.; Kawasumi, M.; Kojima, Y.; Okada, A.; Kurauchi, T.; Kamigaito, O. J Mater Res 1993, 8, 1174.
3. Usuki, A.; Kojima, Y.; Kawasumi, M.; Okada, A.; Fukushima, Y.; Kurauchi, T.; Kamigaito, O. J Mater Res 1993, 8, 1179.
4. Kojima, Y.; Usuki, A.; Kawasumi, M.; Okada, A.; Kurauchi, T.; Kamigaito, O. J.; Polym Sci Part A: Polym Chem 1993, A31, 983.
5. Kawasumi, M.; Hasegawa, N.; Kato, M.; Usuki, A.; Okada, A. Macromolecules 1997, 30, 6333.
6. Kato, M.; Usuki, A.; Okada, A. J Appl Polym Sci 1997, 63, 1781.
7. Hasegawa, N.; Kawasumi, M.; Kato, M.; Usuki, A.; Okada A. J Appl Polym Sci 1998, 67, 87.
8. Wang, Y.; Chen, F.-B.; Wu, K.-C.; Wang, J.-C. Polym Eng Sci 2006, 46, 289.
9. Lertwimolnun, W.; Vergnes, B. Polymer 2005, 46, 3462.
10. Perrin-Sarazin, F.; Ton-That, M.-T.; Bureau, M. N. Denault, J. Polymer 2005, 46, 11624.
11. Hong, C. H.; Lee, Y. B.; Bae, J. W.; Jho, J. Y.; Nam, B. U.; Hwang, T. W. J Appl Polym Sci 2005, 98, 427.
12. LeBaron, P. C.; Wang, Z.; Pinnavaia, T. J. Appl Clay Sci 1999, 15, 11.
13. Vashi, P. N.; Kulshreshtha, A. K.; Dhake, K. P. J Apppl Polym Sci 2003, 87, 1190.
14. Willis, J. M.; Favis, B. D. Polym Eng Sci 1988, 28, 1416.
15. Willis, J. M.; Favis, B. D.; Lavallee, C. J. J Mater Sci 1993, 28, 1749.
16. Van Gheluwe, P.; Favis, B. D.; Chalifoux, J.–P. J Mater Sci 1988, 23, 3910.
17. Vallejo, F. J.; Eguiazabal, J. I.; Nazabal, J. Polymer 2000, 41, 6311.
18. Montoya, M.; Abad, M. J.; Barral, L.; Bernal, C. Eur Polym J 2006, 42, 265.
19. Montoya, M.; Abad, M. J.; Barral Losada, L.; Bernal, C. J Appl Polym Sci 2005, 98, 1271.
20. Abad, M. J.; Ares, A.; Barral, L.; Cano, J.; Díez, F. J.; García-Garabal, S.; López, J.; Ramírez, C. J Appl Polym Sci 2004, 94, 1763.
21. Shah, R. H.; Hunter, D. L.; Paul, D. R. Polymer 2005, 46, 2646.
22. Shah, R. K.; Paul, D. R. Macromolecules 2006, 39, 3327.
23. Chisholm, B. J.; Moore, R. B.; Barber, G.; Khouri, F.; Hempstead, A.; Larson, M.; Olson, E.; Kelley, J.; Balch, G.; Caraher, J. Macromolecules 2002, 35, 5508.
24. Barber, G. D.; Calhoun, B. H.; Moore, R. B. Polymer 2005, 46, 6706.
25. Lee, J. A.; Kontopoulou, M.; Parrent, J. S. Polymer 2005, 46, 5040.
26. Parent, J. S.; Liskova, A.; Resendes, R. Polymer 2004, 45, 8091.
27. Sanchez-Valdes, S.; Lopez-Quintanilla, M. L.; Ramirez-Vargas, E.; Medellin-Rodriguez, F. J.; Gutierrez-Rodriguez, J. M. Macromol Mater Eng 2006, 291, 128.
28. Hotta, S.; Paul, D. R. Polymer 2004, 45, 7639.
29. Morgan, A. B.; Gilman, J. W. J. Appl Polym Sci 2003, 87, 1329.

30. Lee, J. W.; Kim, M. H.; Choi, W. M.; Park, O. O. J Appl Polym Sci 2006, 99, 1752.
31. Lertwimolnum, W.; Vergnes, B. Polym Eng Sci 2006, 46, 314.
32. Galgali, G.; Ramesh, C.; Lele, A. Macromolecules 2001, 34, 852.
33. Solomon, M.; Almusallam, A. S.; Seefeldt, K. F.; Somwangthanaroj, A.; Varadan, P. Macromolecules 2001, 34, 1864.
34. Si, M.; Araki, T.; Ade, H.; Kilcoyne, A. L. D.; Fisher, R.; Sokolov, J. C.; Rafailovich, M. H. Macromolecules 2006, 39, 4793.
35. Ray, S. S.; Pouliot, S.; Bousmina, M.; Utracki, L. A. Polymer 2004, 45, 8403.
36. Ray, S. S.; Bousimina, M. Macromol Rapid Commun 2005, 26, 450.
37. Ray, S. S.; Bousimina, M. Macromol Rapid Commun 2005, 26, 1639.
38. Ray, S. S.; Bousimina, M.; Maazouz, A. Polym Eng Sci 2006, 46, 1121.
39. Krishnamoorti, R.; Giannelis, E. P. Macromolecules 1997, 30, 4097.
40. Rosedale, J. H.; Bates, F. S. Macromolecules 1990, 23, 2329.
41. Larson, R. G.; Winey, K. I.; Patel, S. S.; Watanabe, H.; Bruinsma, R. Rheol Acta 1993, 32, 245.